Effects of Delamination Shapes, Sizes, Locations, and Boundary Conditions Using Modal Analysis of Composite Structure

Nitesh Talekar

Research Scholar Ph.D, Visveswaraya National Institute of Technology

Email: kitsniteshtalekar@gmail.com

Mangesh Kotambkar

Associate Professor, Visveswaraya National Institute of Technology

Email: mskotamb@gmail.com ORCID: **0000-0002-6075-9663**

Kiran Kaware (Corresponding Author)

Assistant Professor, Sandip University, Nashik

Email: kiran.kaware@gmail.com ORCID: **0000-0002-0087-757X**

Akshay Sontakkey

Research Scholar Ph.D, Visveswaraya National Institute of Technology

Email: akshay.sontakke728@gmail.com ORCID:**0000-0002-6154-8534**

Abstract

Fiber-reinforced polymer composites offer numerous advantages over conventional materials, due to their better specific strength and stiffness. The service conditions and manufacturing process of the laminated plate are the causes of delamination which is a critical issue that needs to be addressed. Localized stress increases in and surrounding the delaminated zone if incipient delamination is not detected and stopped. This accelerated delamination process, driven by localized stress, ultimately leads to the failure of the composite structure. Therefore, it is imperative to explore the dynamic characteristics of delaminated composite structures. This study focuses on assessing the impact of delamination at various interfaces on the vibration characteristics of composite square plates composed of multiple plies. It also investigates how factors such as the shape, severity, and location of delamination affect the vibration properties of the composite plate. The modal analysis results obtained from a Finite Element (FE) model created using ABAQUS software are compared and validated against analytical and experimental findings from prior literature. Additionally, an analytical model used for finite element modeling of the composite plate is presented. The findings reveal that modal parameters of delaminated plates can serve as valuable indicators for identifying the shape, severity, and location of delamination.

Keywords – Delamination, Natural frequency, composite plate, free vibration

1 Introduction:

Composite materials are progressively supplanting traditional metals within the engineering domain due to their superior combination of high specific strength and stiffness. These materials exhibit versatility, enabling them to conform to various shapes, offer corrosion resistance, and possess the potential to address future challenges by potentially substituting existing materials. The primary types of damage observed in composite materials include inter-laminar de-bonding, micro-buckling, micro-cracks, delamination, and the presence of foreign inclusions. Typically, these internal damages arise either during the manufacturing processes or as a result of service conditions. They remain inconspicuous on the surface, residing within the layered structures. Among these, de-bonding or delamination is a form of hidden damage that is both prevalent and highly detrimental in composite structures However, their presence significantly reduces the stiffness as well as strength of the structure [1][2]–[4] and also affects the vibration characteristics of the structure [5][6]. The direct reduction in stiffness and hence natural frequency may match the working frequency resulting in resonance. Therefore, it is necessary to study the dynamic behavior of delaminated structures.

Damage identification method includes non-destructive testing: magnetic field methods, acoustic or ultrasonic methods, radiography or thermal field, and eddy-current method [7]. The modal parameters depend on the physical properties of the structures. Therefore, a reduction in stiffness due to the loosening of plies or the initiation of cracks will cause considerable changes in the modal properties. Changes in modal properties are being used as an indicator of the damage. Vibration-based defect detection simplifies into the realm of pattern recognition, as outlined in reference [8]. The measurement of natural frequency offers reliability and ease of assessment, being a straightforward single-point measurement. Nevertheless, while a shift in frequency effectively detects the presence of damage or multiple damages, determining their precise location and assessing their severity remains a challenging task, as discussed in reference [9].

Methods to detect, locate, and identify damage in structure by exploring changes in vibration response measured were summarized by S. Doebling [8]. C. Della et. al [10] studied the delamination effect on the free vibration frequency and the mode shapes of a layered composite plate.

Zhifang Zhang et. al [9] solved the non-linear equation by using a different inverse algorithm to predict the size, interface and location of delamination those are direct solutions using an artificial neural network (ANN), graphical method, and surrogate-based optimization. M. Shariati Nia et. al [5] determined the delaminated composite beam natural frequencies from both free and constrained mode frequencies. R. Palazzetti et.al [11] proposed a novel concept for delamination monitoring in composites based on a nonlinear signal correlation. Experiments are performed on undamaged and delaminated beams and their free decay response is used. Experiments show that the proposed method accurately detects and localizes delamination in the composite beam. David Garcia et.al [12] used Multichannel Singular Spectrum Analysis (MSSA) for structural health monitoring. Vibration response signals are recorded by an accelerometer from damaged and healthy laminated composite beams.

K. Alnefaie [6] proposed a new model to detect delamination in the composite plate. As per the author, the effect of delamination is easier to identify on mode shapes than it is on the natural frequencies. Shih-Yao K [13] investigated the delamination effect on natural frequencies of simply supported rectangular angle ply and cross-ply laminates using the finite strip method. The delamination effect on the natural frequency increases with delamination length. R Sultan et. al [7] studied free vibration testing of square composite plates with different areas of artificial delamination. Delamination in a laminated plate reduces its natural frequencies and reduction increases when the delamination area increases. The effect of the delamination area on the first mode is very small. The higher natural frequency modes are significantly influenced by the delamination area.

Israr Ullah et.al [14] suggested vibration responses delamination identification in the layer structure when excited at the lower modes. Roberto Palazzetti et.al [11] investigated a vibration-based structural health monitoring (VSHM) method to find delamination in the laminate composite beam. Guechaichia et.al [15] suggested a novel non-model-based method for composite beams that utilizes only the fundamental frequency of the beam to find and locate damage. R. Sultan et.al [16] conducted FE modeling to simulate the dynamics of composite plates with delamination and to extract their vibration parameters.

Some other findings on composite plates and beams showed that small-size delamination does not remarkably affect the lower mode of vibration [17][18][19]–[21]. Zak et al.[22] experimentally verified the above result with single-edge delamination on cantilever beams and plates. Jian et al. [23] investigated experimentally that a unidirectional composite plate made of glass fiber with circular mid-plane delamination showed that small (0.34 % of plate area) mid-plane delamination significantly affected the first seven frequencies and reduction in the natural frequency is more noticeable at higher modes. Various experimental investigation showed similar results[24][25][26][27][28]. However, Penn et al.[29] studied thick composite plate experimentally that, the first six modes of vibration were not remarkably affected by small size delamination (size of less than 13% of the plate area).

Delamination location also affects the dynamic response of the plate. It was found that the location of the mid-plane delamination near the fixed side of the composite plate reduces the natural frequency most [30][31][25][32]. The presence of delamination causes mode shape change of the composites and it is investigated experimentally[33][34]. Also, the non-linearity in mode shape is observed which may be caused by either delamination breathing or delaminated layers contact during vibration or both. An experimental study by Shen and Grady [35] and Lestari and Hanagud [36] showed the nonlinearity in the mode shapes by delamination breathing. However, for small delamination, breathing has little effect on the natural frequencies of low vibration modes [29] [34][38].

Multiple delamination studies showed a reduction in natural frequency with the increasing number of delamination[39][40][18][24][41]. However, a single long delamination effect is more remarkable than multiple delamination effect with sufficient length present along the alike axial direction. Shu and Della [42][43] and Della et al. [44][45] examine the second delamination effect on the mode shape and natural frequency of the beam. It is observed that second long delamination significantly influences whereas second short delamination is less significant on the natural frequency.

The effect of delamination shape and its severity is the scope of the above studies and therefore various shapes and effects of its location on the natural frequency are studied. The present study also presents a mathematical model for the dynamics of delaminated composite laminates. Presence of multiple delamination and non-linearity is the future scope of this study.

2 Material Model

Three translational DOFs at each node along the global coordinate axes of x, y, and z are used in the FE model of the eight-node element. The element thickness is selected as the thickness of individual lamina. The fiber direction is coincident with the first axis. x_1, x_2, and x_3 are arranged as a local element coordinate system. All the elements have identical elemental physical parameters. So, the Elemental displacement field is given by

$$\{\delta\} = (u, v, w)^T = \sum_{i=1}^{8}[N_i]\,\{\delta i\} \tag{1}$$

Where,$\{\delta\} = (u_i, v_i, w_i)^T$ is the nodal displacement vector at a node i and N_i is the shape function.Then the elemental strain vector expressed in terms of global coordinate displacement as

$$\{\varepsilon^e\} = (\varepsilon_{11}^e, \varepsilon_{22}^e, \varepsilon_{33}^e, \varepsilon_{12}^e, \varepsilon_{13}^e, \varepsilon_{23}^e)^T = \sum_{i=1}^{8}[B_i]\{\delta i\} \tag{2}$$

$$[Bi] = [\Delta][Ni] \tag{3}$$

and

$$[\Delta] = \begin{bmatrix} \frac{\partial}{\partial x} & 0 & 0 \\ 0 & \frac{\partial}{\partial y} & 0 \\ 0 & 0 & \frac{\partial}{\partial z} \\ \frac{\partial}{2\partial y} & \frac{\partial}{2\partial x} & 0 \\ 0 & \frac{\partial}{2\partial z} & \frac{\partial}{2\partial y} \\ \frac{\partial}{2\partial z} & 0 & \frac{\partial}{2\partial z} \end{bmatrix} \tag{4}$$

Thus, the elemental strain vector can be expressed in terms of nodal displacements as $\{\varepsilon^e\} = [B]\{\delta^e\}$

$$[B] = [[B_1], [B_2], \dots, [B_8]] \text{and} \{\delta^e\} = (\{\delta_1\}^T, \dots, \{\delta_8\}^T)^T \tag{5}$$

Therefore, the global coordinate system elemental stresses expressed in term of nodal displacement as

$$\{\sigma^e\} = \{\sigma_{11}^e, \sigma_{22}^e, \sigma_{33}^e, \sigma_{12}^e, \sigma_{13}^e, \sigma_{23}^e\} = \sum_{i=1}^{8}[K^e]\{\delta^e\} \tag{6}$$

Where, $[K^e]$is the elemental stiffness matrix, $[K^e] = \int_{v_e}[B]^T[A][C][A]^{-1}[B]dV$ (7)

Where

ISSN: 0067-3064

$$[C]=\begin{bmatrix}\frac{1}{E_1} & \frac{-\vartheta_{12}}{E_1} & \frac{-\vartheta_{13}}{E_1} & 0 & 0 & 0\\ \frac{-\vartheta_{12}}{E_1} & \frac{1}{E_2} & \frac{-\vartheta_{23}}{E_2} & 0 & 0 & 0\\ \frac{-\vartheta_{13}}{E_1} & \frac{-\vartheta_{23}}{E_2} & \frac{1}{E_3} & 0 & 0 & 0\\ 0 & 0 & 0 & \frac{1}{G_{12}} & 0 & 0\\ 0 & 0 & 0 & 0 & \frac{1}{G_{13}} & 0\\ 0 & 0 & 0 & 0 & 0 & \frac{1}{G_{23}}\end{bmatrix}^{-1} \tag{8}$$

Is material constants matrix, where$E_1, E_2, E_3, G_{12}, G_{13}, G_{23}, \vartheta_{12}, \vartheta_{13}, \vartheta_{23}$being the individual lamina orthotropic elastic constants, and

$$[A]=\begin{bmatrix}cos^2\Theta & sin^2\Theta & 0 & 0 & 0 & -sin2\Theta\\ sin^2\Theta & cos^2\Theta & 0 & 0 & 0 & sin2\Theta\\ 0 & 0 & 1 & 0 & 0 & 0\\ 0 & 0 & 0 & cos\Theta & sin\Theta & 0\\ 0 & 0 & 0 & -sin\Theta & cos\Theta & 0\\ sin\Theta cos\Theta & -sin\Theta cos\Theta & 0 & 0 & 0 & cos2\Theta\end{bmatrix} \tag{9}$$

is local and global coordinate transformation matrix. Then, kth elemental strain energy is given by

$$U_k^e=\frac{1}{2}\int_{v_k}\{\varepsilon^e\}^T\{\sigma^e\}dV=\frac{1}{2}\{\delta_k^e\}^T[K_k^e]\{\delta_k^e\} \tag{10}$$

Where $[K_k^e]$ and $\{\delta_k^e\}$ represents kth elemental stiffness matrix and the displacement vector, respectively.

For a composite plate comprising of N elements, the total strain energy is as

$$U=\sum_{k=1}^N U_k^e=\frac{1}{2}\sum_{k=1}^N\{\delta_k^e\}^T\,[K_k^e]\{\delta_k^e\} \tag{11}$$

Therefore, after assembling all the elemental nodal displacements, the total strain energy of a multi-plies composite plate is written as

$$U=\frac{1}{2}\{\delta\}^T[K]\{\delta\} \tag{12}$$

Where$[K]$and$\{\delta\}$are the global nodal stiffness matrix and displacement vector, respectively. Similarly, the kth elemental kinetic energy is

 ISSN: 0067-3064

$$T_k^e = \frac{1}{2}\int_{v_k} \rho \{\dot{\delta}_k^e\}^T dV = \frac{1}{2}\{\dot{\delta}_k^e\}^T [M_k^e]\{\dot{\delta}_k^e\} \tag{13}$$

Where$[M_k^e]$and$\{\dot{\delta}_k^e\}$ represents kth elemental mass matrix and the velocity vector, respectively.

For a composite plate comprising of N elements, the total kinetic energy is as

$$T = \sum_{k=1}^{N} T_k^e = \frac{1}{2}\sum_{k=1}^{N}\{\dot{\delta}_k^e\}^T [M_k^e]\{\dot{\delta}_k^e\} \tag{14}$$

Therefore, after assembling all the elemental nodal velocities, the total kinetic energy of a multi-plies composite plate is written as

$$T = \frac{1}{2}\{\dot{\delta}\}^T [M]\{\dot{\delta}\} \tag{15}$$

where $[M]$ and $\{\dot{\delta}\}$ are the global nodal mass matrix and velocity vector, respectively.

The kinetic energy of the composite laminate in the case if plate experiences ω angular frequency harmonic motion is

$$T = \frac{1}{2}\omega^2\{\delta\}^T [M]\{\delta\} \tag{16}$$

Then, the free vibration equation of motion for the plate by Lagrange's principle is converted to the eigen value problem

$$([K] - \omega^2[M])\{\delta\} = 0 \tag{17}$$

Therefore, natural frequenciesω_i, modal strains, mode shape and all the other modal parameters are obtained.

To ensure the material continuity to an arbitrary intact laminated plate, for each pair of coincident nodes, the movement and their change on the lower and the upper adjacent lamina have to be equal in the computing process. For the delaminated region, pairs of nodes are modeled where delamination is to be induced. Within the delamination region, the pairs of nodes are not attached and their lower and upper surface displacements are not to be connected.

3 Finite Element modeling

The following sections describe the FE modeling of composite structures for different laminas.

3.1 FE Model of unidirectional composite laminate with eight-lamina

In order to verify the precision of the modal analysis findings, an evaluation of element sensitivity is carried out. This evaluation focuses on an eight-lamina composite square plate, featuring a side length of 178 mm and a lamina thickness of 0.1975 mm. All plies in the composite have a fiber orientation angle of 0°, and the material constants are utilized as, E_1 = 172.7 GPa, $E_2 = E_3$ = 7.2 GPa, $G_{12} = G_{13}$ = 3.76 GPa, G_{23} = 2.71 GPa, $\vartheta_{12} = \vartheta_{13}$ = 0.3 and ϑ_{23} = 0.33and ρ =1566 kg/m^3[46] and [47].

Table 1 displays the natural frequencies of the first six vibration modes for various mesh sizes. The findings exhibit a high degree of conformity with the reference results provided in [4]. Notably, as the number of elements per layer escalates from 200 to 2500, a significant enhancement in accuracy becomes apparent. However, surpassing the threshold of 2500 elements does not yield further improvements in result precision. Consequently, 2500 elements per layer are deemed optimal. To bolster confidence in the model, Table 2 compares the modal analysis results obtained with 2500 elements per layer against additional references. The numerical results from the present model exhibit a notably closer concordance with the numerical results of Alnefaie [6], Yam et al. [46] and experimental work of Lin et al. [47] than their numerical results.

Table 1 Natural frequency (Hz) of free healthy plate [0°/0°/0°/0°]$_S$ using different mesh sizes

Mode	Natural Frequency in Hz for number of element per ply						
	200		400		900		2500
	Present	Alnefaie[6]	Present	Alnefaie[6]	Present	Alnefaie[6]	Present
1	81.81	81.36	81.72	81.48	81.58	81.56	81.55
2	110.75	109.5	110.31	109.2	110.00	109.58	109.96
3	201.33	200.84	200.59	199.5	199.89	199.51	199.77
4	311.68	298.13	307.13	300.46	303.86	301.73	303.46
5	401.46	396.95	396.71	391.4	393.17	391.12	392.68
6	541.66	530.36	539.47	533.89	537.87	535.8	537.67

Table 2 Natural frequency (Hz) of free healthy plate [0°/0°/0°/0°]s

Mode	Present	Alnefaie[6]	Yam et al. [46]	Lin et al. [47]	
		Numerical	Numerical	Numerical	Experimental
1	81.55	81.48	82.26	83.57	81.50
2	109.96	109.2	113.1	118.42	107.4
3	199.77	199.5	207.29	207.79	196.6
4	303.46	300.46	325.28	329.41	285.5
5	392.68	391.4	408.51	419.83	382.5
6	537.67	533.89	539.92	546.93	531.00

3.2 FE Model of cross ply composite laminate with sixteen-lamina

In addition to the above model, a new model with sixteen-layer free plate of the total thickness of 0.08 and an area of 240 × 180 mm^2 is selected for verification. The plies are oriented as [0°/0°/90°/90°/0°/0°/90°/90°]s and the constants are E_1 = 125 GPa, E_2 = E_3 = 8.5 GPa, G_{12} = G_{13} = 4.5 GPa, G_{23} = 3.27 GPa, $\vartheta_{12} = \vartheta_{13} = \vartheta_{23} = 0.3$ and ρ = 1550 kg/m^3, Wei et al. [48].

The first six produced natural frequencies are compared with the results of numerical and experimental model by Wei et al. [48] shown in table 3. Present results demonstrate better consent with the experimental results than the analytical results reported which again validate the current FE model.

Table 3 Natural frequency (Hz) of free intact plate [0°/0°/90°/90°/0°/0°/90°/90°]s

Mode		Alnefaie[6]	Wei et al. [48]	
	Present	Numerical	Numerical	Experimental
1	88.344	89.16	90.52	90
2	280.9	278.97	279.17	289
3	332.71	330.35	333.59	318
4	356.13	354.92	354.22	354
5	397.42	393.26	397.62	386
6	580.32	574.5	583.71	570

4 Result and Discussion

4.1 Effect of Delamination Size and Location

The validated finite element model mentioned above is subsequently employed for assessing delamination effects. This involves the analysis of a square plate made of glass fiber/epoxy material, measuring 15.2 cm in side length, and featuring a unidirectional orientation at 0 degrees. The plate is clamped at one end and others ends are free. Delamination of thickness 61µm [23] and the desired area of 10%, 20%, 30%, 40% and 50% (as shown in fig. 1) were created in the middle interface of each plate. Which means that in a 2-ply composite plate, delamination is created in between interface of first and second ply. Whereas, in 4-ply composite, it is in between second and third ply. Likewise, for an 8-ply plate, it is in between fourth and fifth ply whereas, for a 16-ply plate, it is in between eighth and ninth ply. Four different delaminationviz.1. Rectangular delamination at the free end (RF), 2. Rectangular delamination at side end (RS), 3. Triangular delamination at the corner (TC) and 4. Square delamination at the corner (SC) is also considered to study the effect of delaminated location. Above plate is then analyzed as four different plies of the plate (2-ply, 4-ply, 8-ply and 16-ply) to study the effect of multiple plies delaminated plate on the free vibration analysis. In every plate, lamina thickness is kept constant which is 0.2975 mm and therefore the total thickness of the plate is then varied. The total thickness of 2-ply, 4-ply, 8-ply and the 16-ply plate is then 0.595 mm, 1.19 mm, 2.38 mm and 4.76 mm respectively. Delamination area for 10%, 20%, 30%, 40% and 50% plate is shown in Table 4. The elastic constants of the unidirectional glass fibre/epoxy composite material for 0.65 fibre volume fraction are considered as [23].

$E_1 = 58.8 \times 10^9$ Pa, $E_2 = E_3 = 17.5 \times 10^9$ Pa, $G_{12} = G_{13} = 7.28 \times 10^9$ Pa, $G_{23} = 6.9 \times 10^9$ Pa, $\vartheta_{12} = \vartheta_{13} 0.265$, $\vartheta_{23} = 0.3$, $\rho = 2042$ kg/m^3.

A fine mesh is employed to conduct the modal analysis of the composite structure. Within the ABAQUS element library, the chosen element is the SC8R: an 8-node quadrilateral in-plane general-purpose continuum shell. This element implements reduced integration along with hourglass control. The fine mesh is utilized to discretize the finite element model, and the global size for the hexahedral element is set at 0.002 cm. For solving the eigenvalue problems in each case studied, the Lanczos eigensolver is applied.

Table 5a, Table 5b, Table 5c and Table 5d shows first ten modal frequency (Hz) of delamination present at RF, RS, TC and SC respectively for 2-ply plate. Similarly, Table 6, 7 and 8 shows first ten modal frequency (Hz) of delamination present at RF (Table a), RS (Table b), TC (Table c) and SC (Table d) for 4-ply, 8-ply, 16-ply plate respectively.

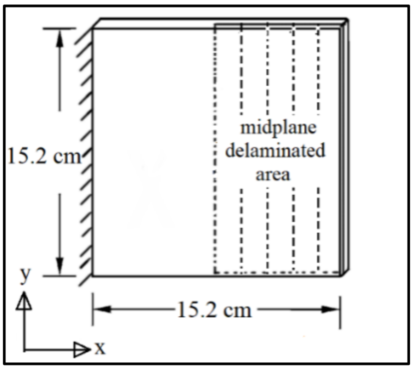

Fig. 1a Rectangular delamination at free end (RF)

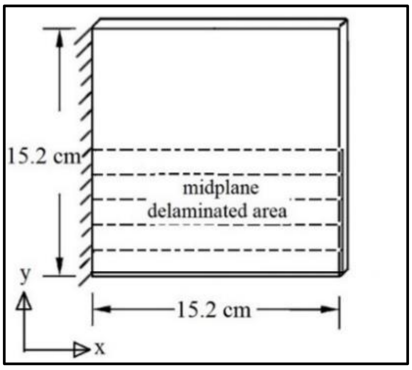

Fig. 1b Rectangular delamination at side end (RS)

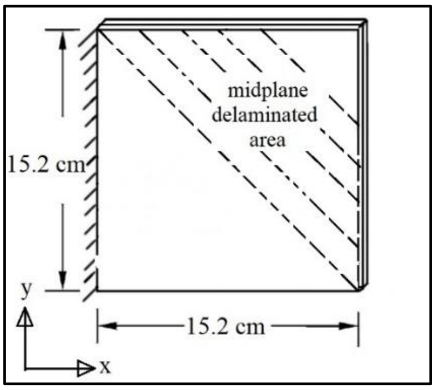

Fig. 1c Triangular delamination at corner (TC)

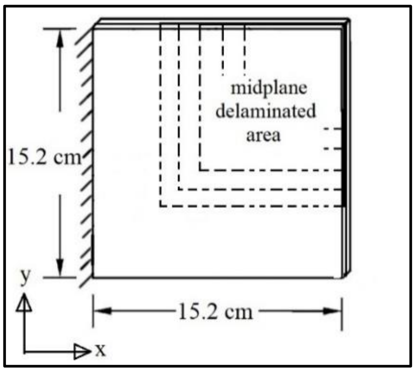

Fig. 1d Square delamination at corner (SC)

Fig. 1 Delamination location and dimension of the plate

Table 4 Delamination area of plate

Sr. No.	Delamination Area (%)	Delamination Area (sq. cm)
1	10%	4.8066
2	20%	6.7976
3	30%	8.3253
4	40%	9.6133
5	50%	10.7480

Table 5a First ten modal frequency (Hz) of delamination present at RF for 2-ply plate

Mode No.	Natural frequency (Hz) for different Delamination area				
	10%	20%	30%	40%	50%
1	22.973	22.391	16.098	9.973	6.4318
2	37.98	37.49	30.464	28.455	25.884
3	98.196	47.574	36.71	35.429	33.053
4	131.98	92.465	83.882	64.401	40.851
5	163.1	148.03	96.277	67.744	51.059
6	186.36	150.33	110.69	74.544	65.8
7	224.6	171.74	123.64	94.855	83.169
8	228.42	198.73	131.59	112.04	103.15
9	339.39	213.12	156.24	120.23	103.17
10	347.81	260.45	165.85	141.13	121.74

Table 5b First ten modal frequency (Hz) of delamination present at RS for 2-ply plate

Mode No.	Natural frequency (Hz) for different Delamination area				
	10%	20%	30%	40%	50%
1	10.956	10.994	10.992	10.93	10.81
2	39.092	37.994	36.758	35.37	32.369
3	66.378	65.536	54.589	40.825	33.792
4	115.94	90.136	64.316	63.197	62.265
5	129.37	99.321	77.657	68.852	64.592
6	191.74	124.75	119.88	115.81	94.615
7	219.02	164.72	150.63	120.94	101.77
8	233.11	189.88	159.17	126.61	109.84
9	244.44	224	182.57	135.49	112.31
10	260.22	232.36	182.6	174.74	170.5

Table 5c First ten modal frequency (Hz) of delamination present at TC for 2-ply plate

Mode No.	Natural frequency (Hz) for different Delamination area				
	10%	20%	30%	40%	50%
1	22.53	22.602	21.796	20.249	18.516
2	39.574	36.961	35.311	30.743	25.233
3	96.735	61.461	43.452	30.824	30.883
4	120.62	82.867	82.503	69.521	69.916
5	122.89	109.5	99.619	92.355	81.672
6	142.78	150.37	147.22	95.661	89.328
7	200.85	168.41	150.97	136.81	113.59
8	233.81	190.79	184.22	137.06	136.31
9	312.51	219.77	196.66	147.75	153.76
10	329.71	272.18	213.79	178.67	177.43

ISSN: 0067-3064

Table 5d First ten modal frequency (Hz) of delamination present at SC for 2-ply plate

Mode No.	Natural frequency (Hz) for different Delamination area				
	10%	20%	30%	40%	50%
1	10.651	10.893	11.153	11.419	12.75
2	38.758	36.099	32.322	29.117	26.967
3	68.175	70.769	47.244	35.465	28.387
4	99.438	73.428	72.87	70.468	66.206
5	117.9	80.692	76.5	76.372	75.355
6	141.09	111.45	110.06	104.52	83.651
7	187.95	170.57	139.24	113.51	120.08
8	210.43	202.93	153.18	139.07	130.13
9	227.37	208.63	194.03	166.28	133.11
10	257.37	220.7	203.6	180.39	165.93

Table 6a First ten modal frequency (Hz) of delamination present at RF for 4-ply plate

Mode No.	Natural frequency (Hz) for different Delamination area				
	10%	20%	30%	40%	50%
1	24.71	24.845	24.801	24.391	23.404
2	61.243	59.848	57.667	54.93	51.792
3	148.02	143.52	129.67	80.972	52.092
4	209.72	190.51	146.51	116.83	89.777
5	214.06	200.28	166.34	122.62	106.18
6	388.65	324.3	184.12	144.73	128.96
7	432.74	363.64	189.42	170.95	161.91
8	451.87	371.61	288.44	207.38	164.69
9	517.57	378.59	320.97	282.58	256.49
10	677.71	391.97	337.69	322.33	283.2

Table 6b First ten modal frequency (Hz) of delamination present at RS for 4-ply plate

Mode No.	Natural frequency (Hz) for different Delamination area				
	10%	20%	30%	40%	50%
1	19.97	19.877	19.632	19.188	18.553
2	60.03	57.334	54.509	52.077	50.075
3	118.28	113.94	108.59	94.872	67.151
4	204.13	191.81	154.49	103.57	99.077
5	213.31	204.76	176.33	152.57	135.47
6	341.79	313.34	185.98	176.06	151.1
7	403.91	324.66	255.45	186.91	169.08
8	418.61	382.98	287.28	268.91	255.16
9	528.74	397.81	349.26	321.79	285.57
10	643.56	436.43	372.1	327.51	304.32

ISSN: 0067-3064

Table 6c First ten modal frequency (Hz) of delamination present at TC for 4-ply plate

Mode No.	Natural frequency (Hz) for different Delamination area				
	10%	20%	30%	40%	50%
1	24.513	24.469	24.143	23.39	22.67
2	62.154	59.686	56.535	51.968	47.132
3	140.03	115.48	79.881	57.871	49.843
4	198.38	136.75	129.66	120.81	114.85
5	216.83	157.29	142.15	133.78	126.22
6	255.55	204.95	193.91	163.12	134.72
7	374.99	325.48	224.09	182.3	176.57
8	395.13	347.62	319.52	255.6	204.63
9	436.33	359.61	332.61	291.4	273.63
10	479.34	387.29	352.01	315.38	293.74

Table 6d First ten modal frequency (Hz) of delamination present at SC for 4-ply plate

Mode No.	Natural frequency (Hz) for different Delamination area				
	10%	20%	30%	40%	50%
1	20.052	20.15	20.17	20.07	20.135
2	61.757	60.464	57.89	54.746	51.948
3	121.09	120.51	90.845	68.222	54.601
4	198.06	136.15	117.79	114.44	111.74
5	205.69	162.12	143.37	135.27	131.05
6	271.39	196.27	188.72	181.82	175.45
7	355.05	340.39	295.9	222.18	177.8
8	373.59	354.55	325.75	259.22	207.46
9	418.77	393.26	331.45	294.1	268.99
10	464.92	443.65	345.17	306.83	293.25

Table 7a First ten modal frequency (Hz) of delamination present at RF for 8-ply plate

Mode No.	Natural frequency (Hz) for different Delamination area				
	10%	20%	30%	40%	50%
1	39.489	39.58	39.52	39.189	38.371
2	110.86	107.67	102.71	96.378	89.494
3	234.53	230.67	219.64	161.01	103.24
4	368.67	338.75	286.8	204.48	159.11
5	402.39	356.63	310.3	219.78	191.73
6	690.15	639.93	312.26	274.07	247.05
7	733.5	658.58	346.42	294.83	284.28
8	773.29	677.12	513.91	371.87	300.18
9	956.83	690.67	598.69	551.72	507.12
10	1213.6	697.11	613.76	571.9	551.45

Table 7b First ten modal frequency (Hz) of delamination present at RS for 8-ply plate

Mode No.	Natural frequency (Hz) for different Delamination area				
	10%	20%	30%	40%	50%
1	37.775	37.494	36.891	35.814	34.274
2	108.17	102.06	95.736	90.37	86.255
3	221.17	210	196.33	183.68	130.96
4	369.03	340.35	315.59	191.7	172.88
5	413.23	397.31	324.03	291.77	252.86
6	631.51	553.8	361.08	317.73	266.18
7	752.27	697.34	451.65	322.33	300.56
8	766.52	697.62	494.15	454.44	427.62
9	1034.2	741.72	634.97	537.47	468.44
10	1166.4	822.41	678.8	581.85	547.74

Table 7c First ten modal frequency (Hz) of delamination present at TC for 8-ply plate

Mode No.	Natural frequency (Hz) for different Delamination area				
	10%	20%	30%	40%	50%
1	39.333	39.13	38.701	37.884	37.032
2	111.72	107.26	101.03	94.114	88.921
3	229.31	221.8	149.09	111.88	91.481
4	361.46	222.73	213.61	204.18	196.2
5	396.76	297.45	267.6	259.36	244.79
6	463.26	369.91	342.97	315.42	255.02
7	661.43	613.44	421.22	318.6	302.03
8	698.22	627.75	576.43	482.56	383.1
9	780.53	674.19	625.89	540.21	510.43
10	915.1	699.48	640.18	583.61	549.73

Table 7d First ten modal frequency (Hz) of delamination present at SC for 8-ply plate

Mode No.	Natural frequency (Hz) for different Delamination area				
	10%	20%	30%	40%	50%
1	38.069	37.992	37.704	37.495	36.344
2	112.3	110.35	106.45	101.58	96.443
3	223.99	217.37	171.52	129.24	103.38
4	373.24	256.71	210.11	205.03	200.01
5	393.28	314.63	279.05	263.87	257.12
6	508.94	366.59	346.63	327.61	309.41
7	652.78	625.55	581.24	438.07	350.45
8	712.3	675.49	600.23	499.92	399.94
9	769.95	727.22	641.69	567.23	535.77
10	909.11	860.24	663.54	600.15	562.25

ISSN: 0067-3064

Table 8a First ten modal frequency (Hz) of delamination present at RF for 16-ply plate

Mode No.	Natural frequency (Hz) for different Delamination area				
	10%	20%	30%	40%	50%
1	75.04	75.102	74.927	74.262	72.759
2	213.89	207.06	196.52	183.13	168.83
3	443.34	436.47	417.16	303.48	195.52
4	702.99	642.15	536.41	389.87	295.46
5	786.49	693.5	589.91	407.78	366.16
6	1311.1	1179	607.61	542.41	494.32
7	1414.7	1248.6	640.99	556.62	537.36
8	1463.9	1275.6	957.41	704.47	577.98
9	1850.5	1312.6	1137.7	1084.5	1046.7
10	1860.3	1333.9	1220.7	1124.1	1051.7

Table 8b First ten modal frequency (Hz) of delamination present at RS for 16-ply plate

Mode No.	Natural frequency (Hz) for different Delamination area				
	10%	20%	30%	40%	50%
1	73.997	73.36	72.068	69.777	66.518
2	208.56	195.92	183.02	172.17	164.01
3	430.32	406.17	376.91	350.13	256.74
4	708.94	649.9	601.61	377.65	327.79
5	813.29	781.47	638.79	561.01	471.07
6	1215.9	1049.1	713.5	593.98	520.55
7	1452.8	1341.4	851.08	634.8	588.82
8	1477.3	1360.7	928.72	850.46	799.51
9	1526.7	1437	1223.1	991.53	866.44
10	2016.8	1526.5	1251.6	1120.6	1053.8

Table 8c First ten modal frequency (Hz) of delamination present at TC for 16-ply plate

Mode No.	Natural frequency (Hz) for different Delamination area				
	10%	20%	30%	40%	50%
1	74.694	74.377	73.364	71.99	70.082
2	215.08	207.1	193.68	180.96	169.93
3	434.66	420.26	294.42	221.77	178.04
4	686.44	449.38	402.83	386.3	370.69
5	773.62	588.68	533.05	513.95	496.31
6	860.5	720.39	664.43	615.9	505.06
7	1253.2	1160.8	820.41	618.38	577.28
8	1346.5	1235.9	1089.9	931.31	747.77
9	1485.9	1310.9	1234.4	1030.7	968.91
10	1785.4	1361.7	1235.1	1128.2	1061.9

ISSN: 0067-3064

Table 8d First ten modal frequency (Hz) of delamination present at SC for 16-ply plate

Mode No.	Natural frequency (Hz) for different Delamination area				
	10%	20%	30%	40%	50%
1	74.675	74.281	73.555	72.201	70.311
2	216.93	212.13	205.12	195.49	185.78
3	435.56	412.12	328.09	247.52	192.42
4	719.23	473.89	403.78	391.94	383.13
5	774.17	606.38	549.44	521.8	510.98
6	958.85	707.25	668.92	629.06	593.24
7	1259.9	1158.2	1104.5	833.6	668.14
8	1383.9	1305	1150.9	988.49	792.86
9	1481.1	1381.7	1237.9	1079.6	1023.7
10	1719.6	1513.1	1309.5	1159.9	1089.4

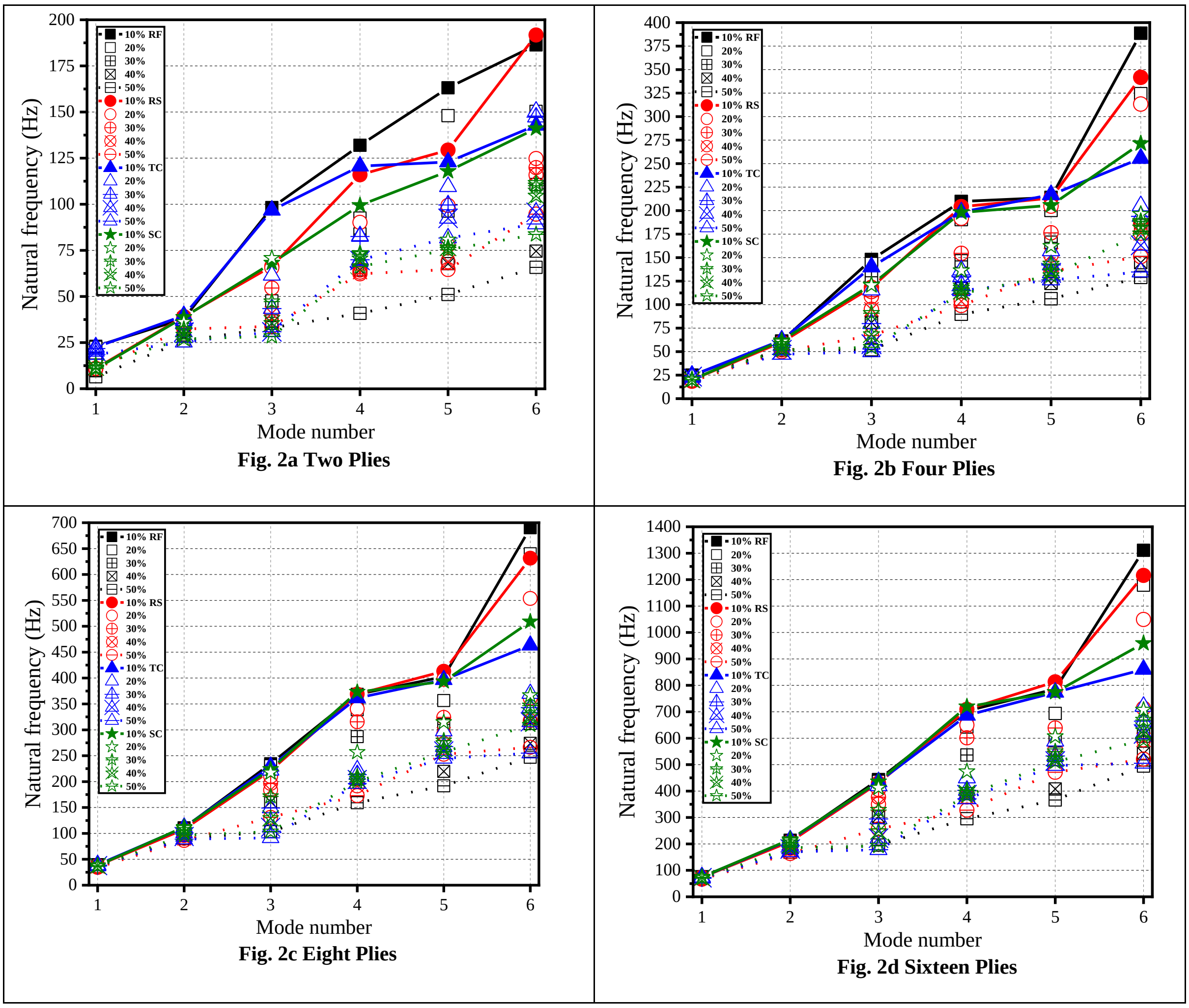

Fig. 2a Two Plies

Fig. 2b Four Plies

Fig. 2c Eight Plies

Fig. 2d Sixteen Plies

Fig.2 First six mode natural frequency of delaminated plate

ISSN: 0067-3064

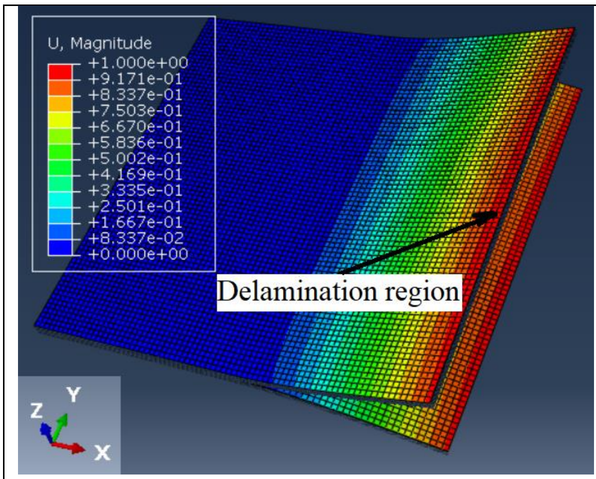

(a) Third mode shape of sixteen plies and 50% rectangular delamination present at free side (195.52 Hz)

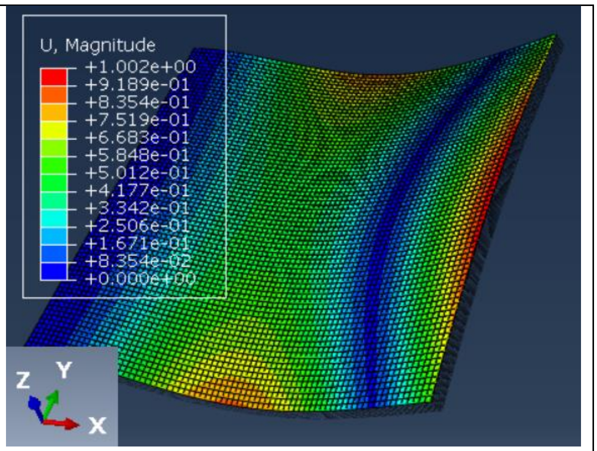

(b) Third mode shape of sixteen plies with no delamination (441.7 Hz)

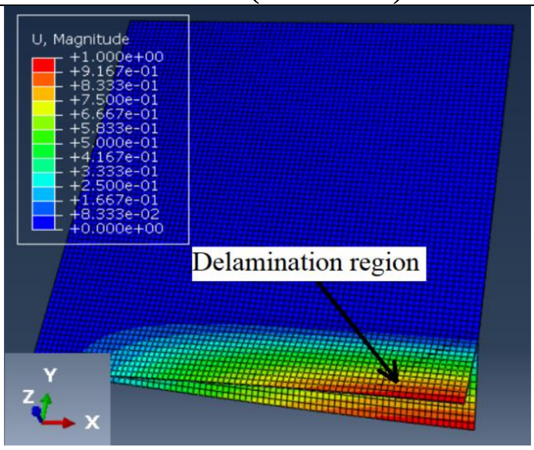

(c) Fourth mode shape of two plies and 40% rectangular delamination present at side end (90.13 Hz)

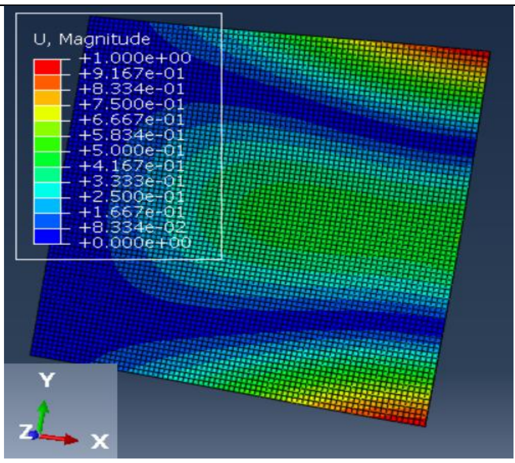

(d) Fourth mode shape of two plies with no delamination (112.15 Hz)

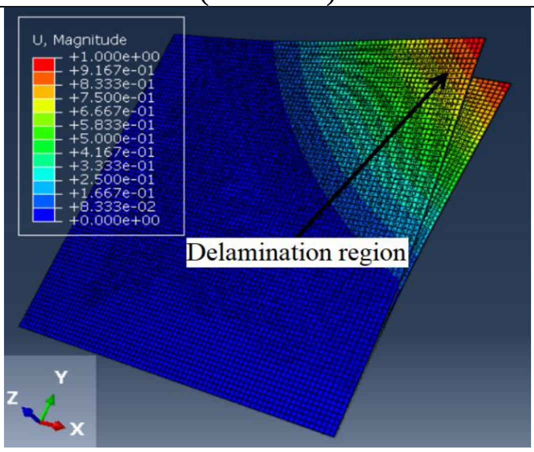

(e) Third mode shape of four plies and 40% triangular delamination present at free corner (57.87 Hz)

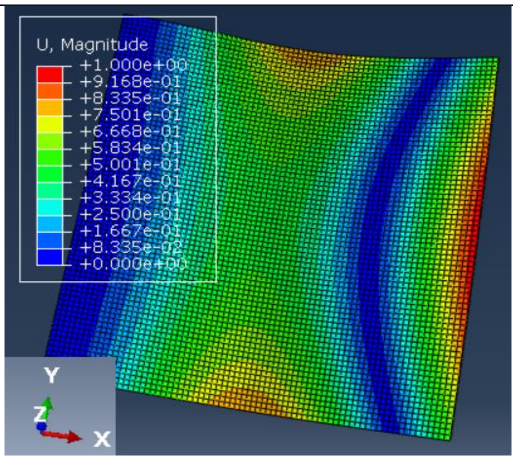

(f) Third mode shape of four plies with no delamination (123.45 Hz)

ISSN: 0067-3064

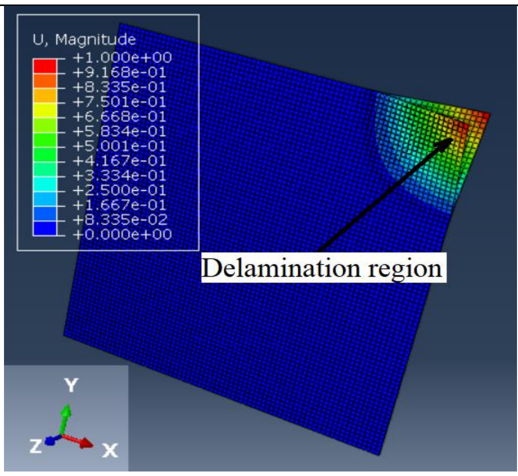

(g) Sixth mode shape of eight plies and 10% square delamination present at free corner (508.94 Hz)

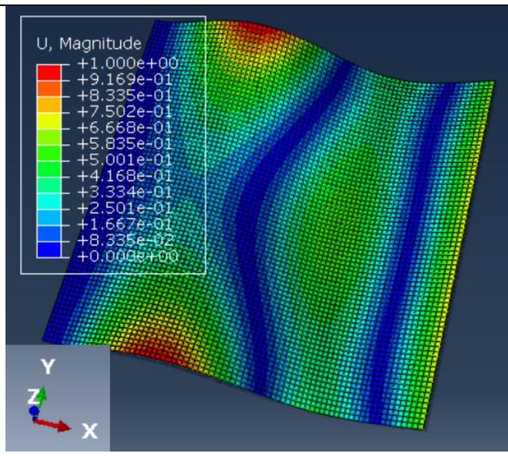

(h) Sixth mode shape of eight plies with no delamination present (674.7 Hz)

Fig. 3 Mode shape of a plate with and without delamination

Generally, the natural frequency is reduced with the presence of delamination which causes a change in mode shape of the composite ply. This happens due to the decrease in the stiffness. For all the boundary condition, Mujumdar and Suryanarayan [30] reported short delamination less than 25% of the length of the beam does not affect much to the first and second mode of vibration. Whereas the effect of long delamination of about 50% of the length of the beam depends on the boundary conditions. In fact, a greater effect on free vibration is caused by more edges restrained of the structure. In a 25% mid-plane delamination in an 8-ply square plate, first 10 mode shapes and natural frequencies do not vary significantly compared to without delaminated plate for all the boundary conditions considered [18].

Fig.2 a, b, c and d represents the graph of first six modes of vibration for two, four, eight and sixteen plies respectively. It is seen that delamination present at the free end is more sensitive compare to all the other location. Generally, higher modes delamination effect is more than that on lower modes is found, but this effect may not continue a routinely increasing fashion with an increase in mode number. It is also proved that a higher number of plies makes the plate stiffer and therefore it's natural frequency increases for all the mode number and delaminated area. It is also obvious that higher delamination area makes plate less stiff and hence its frequency of vibration reduces. For a delaminated plate, as delamination location changes from RF to SC for increasing delamination area, narrowing the graph with mode number. Which means that rectangular delamination present at the free end is most sensitive to delamination area and delamination present at the corner are least sensitive with initial modes

ISSN: 0067-3064

of vibration. Fig. 3 shows modes of vibration with and without delamination. Presence delamination affects the mode shape of the plate can be observed. Therefore, Mode shape of the plate with and without delamination can be analyzed to identify the presence of delamination, its location and severity.

Fig.4 shows a fundamental natural frequency for various plies and location. It is seen that 2 ply plate with delamination present at the free end is having more drop in the frequency when mid-plane delamination increases more than 20%. 16-ply delaminated plate affect free vibration in between triangular delamination and square delamination present at corner end. Effect of delamination geometry present at the corner of the plate reduces with increase in plies number in the plate.

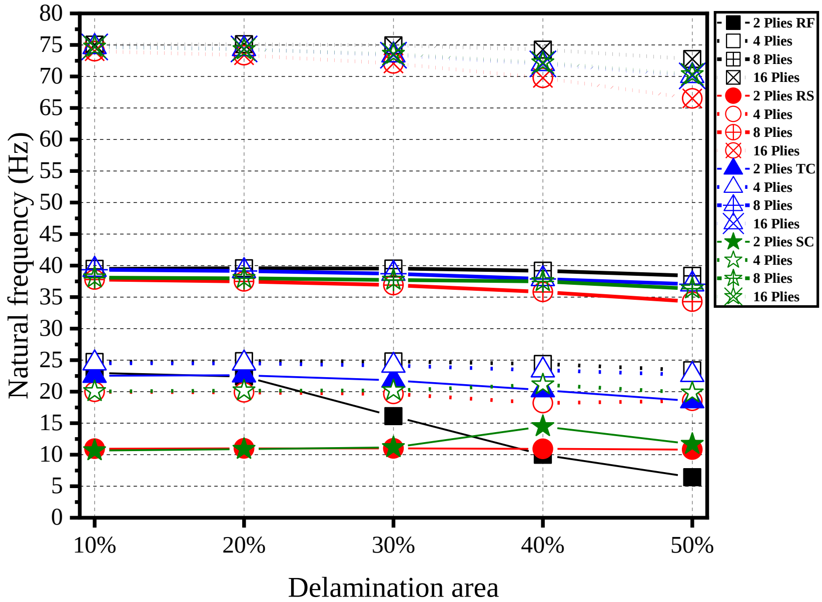

Fig. 4 Fundamental natural frequency for various plies and location

4.2 Effect of Interface and Boundary Condition

Being all the condition, geometry and material properties are the same, interface and boundary condition effect is also studied. To analyze the interface effect, four interfaces (shown in fig. 5) are considered. The figure shows the ply configuration of an 8-ply plate with four interfaces. Natural frequencies are computed for a 10% delamination present at the free end but at one of the interfaces 1, 2, 3 or 4 as shown in fig. 6. Free vibration effect of square delamination present at the centre but at the various interface is studied by F. Ju et.al [18]. Fig. 6 shows natural frequencies (Hz) of CFFF (clamped-free-free-free) 8-plies plate $[0^0/0^0/0^0/0^0]_S$ with a 10% rectangular delamination present at the free end at different interfaces. For a given boundary condition and arrangement, natural frequencies formid-plane delamination is least and increases when the delamination interface moves to the surface of the plate. It is also seen that the rate of increase in frequency is also increased when delamination interface changes from 1 to 4 for all the lower modes of vibration. To study boundary condition effect, four boundary conditions viz. 1. All clamped (CCCC) 2. All simply supported (SSSS) 3. Clamped-free-free-free (CFFF) and 4. All free (FFFF) are considered. Fig. 7 shows natural frequencies of eight plies composite plate $[0^0/0^0/0^0/0^0]_S$ with a 10% rectangular delamination present at free end with various boundary condition for the first five modes. Results behavior are exactly matching with the result produced by F. Ju et.al [18]. More edge restrained of a plate causes more delamination effect on the vibration characteristics is found.

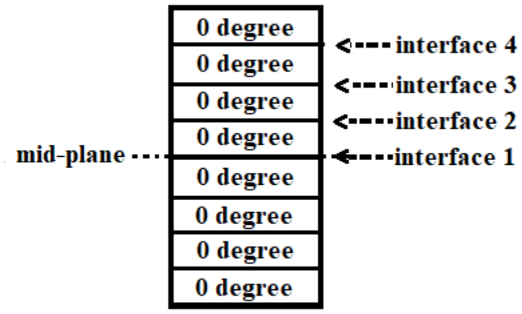

Fig.5 ply configuration of eight plies composite plate

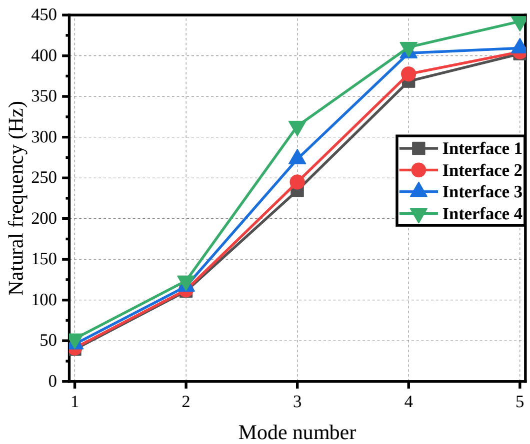

Fig. 6 Natural frequencies (Hz) of CFFF eight plies plate $[0^o/0^o/0^o/0^o]_S$ with a 10% delamination present at free end at different interfaces

ISSN: 0067-3064

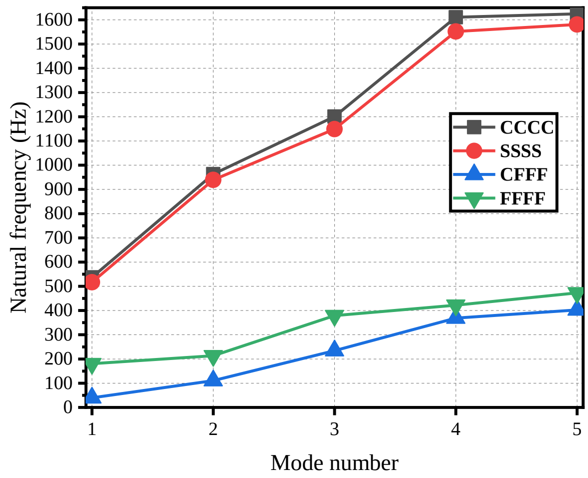

Fig. 7 Natural frequencies (Hz) of composite plates with boundary condition for first five modes

5 Conclusion

A FE formulation is studied for the free vibration characteristics of the composite plate. The research incorporates the selection of various cases from existing literature to enhance the model, which is subsequently validated against both numerical and experimental data. Additionally, the analysis explores the impact of delamination at multiple interfaces. It presents changes in the mode shapes with and without delamination. Results showed that the modal parameters delamination effect of the plate depends not only on location, size, and number of plies but also on the mode number and interface.

The examination reveals that a plate with delamination, which is restrained along its edges, exhibits higher natural frequencies. Additionally, the study concludes that as the number of plies with mid-plane delamination in the plate increases, the range of variation in modal natural frequencies also increases. Mid-plane delamination location considered in the study shows that higher modes of vibration are most affected when delamination is present at the free end and least affected when it is at a corner.

The study can be extened to test low vecity impacted specimen by modal analysis as interlaminater damage in case of low velocity impact is it not easily identifiable.

References

[1] A. C. Garg, “Delamination - a damage mode in composite structures,” *Eng Fract Mech*, vol. 29, no. 5, pp. 557–584, 1988.

[2] T. E. Tay, “Characterization and analysis of delamination fracture in composites: An overview of developments from 1990 to 2001,” *Appl Mech Rev*, vol. 56, no. 1, 2003, doi: 10.1115/1.1504848.

[3] K. Kaware, M. Kotambkar, A. Sontakkey, and N. Talekar, “Finite element analysis of CFRP composite under low velocity impact to improve the impact strength,” *International Journal of Crashworthiness*, vol. 0, no. 0, pp. 1–15, 2022, doi: 10.1080/13588265.2022.2123178.

[4] K. Kaware and M. Kotambkar, “Low velocity impact response and influence of parameters to improve the damage resistance of composite structures/materials: a critical review,” *International Journal of Crashworthiness*, vol. 27, no. 4, pp. 1232–1256, 2022, doi: 10.1080/13588265.2021.1914985.

[5] M. Shariati Nia, K. Torabi, and M. Heidari-rarani, “Free vibration analysis of a composite beam with single delamination- An improved free and constrained model,” *Engineering Solid Mechanics*, vol. 2, pp. 313–320, 2014, doi: 10.5267/j.esm.2014.7.002.

[6] K. Alnefaie, “Finite element modeling of composite plates with internal delamination,” *Compos Struct*, vol. 90, pp. 21–27, 2009, doi: 10.1016/j.compstruct.2009.01.004.

[7] R. Sultan, S. Guirguis, M. Younes, and E. El-Soaly, “Delamination detection of composite laminates using natural frequency vibration method,” *International Journal of Mechanical Engineering and Robotics Research*, vol. 1, no. 2, pp. 286–296, 2012.

[8] S. W. Doebling, C. R. Farrar, and M. B. Prime, “A summary review of vibration-based damage identification methods,” *The Shock and Vibration Digest*, vol. 30, pp. 91–105, 1998.

[9] Z. Zhang, K. Shankar, T. Ray, E. V Morozov, and M. Tahtali, “Vibration-based inverse algorithms for detection of delamination in composites,” *Compos Struct*, vol. 102, pp. 226–236, 2013, doi: 10.1016/j.compstruct.2013.03.012.

[10] C. N. Della and D. Shu, “Vibration of delaminated composite laminates : A review,” *Appl Mech Rev*, vol. 60, pp. 1–20, 2007, doi: 10.1115/1.2375141.

[11] R. Palazzetti, I. Trendafilova, A. Zucchelli, and G. Minak, “Delamination localization and length estimation in composite laminate beam by VSHM and pattern recognition methods,” *14th European Conference on Composite Materials*, 2010.

[12] D. Garcia and I. Trendafilova, “Multivariate statistical analysis for damage and delamination detection in composite structures,” *11th International Conference on Vibration Problems*, 2013.

[13] S. Kuo, “Effect of delamination on natural frequencies of rectangular laminates,” *Jouurnal of Aeronautics, Astronautics and Aviation, Series A*, vol. 43, no. 3, pp. 209–218, 2011.

[14] I. Ullah and J. K. Sinha, “A novel method for delamination detection in composites,” *Int J Innov Appl Stud*, vol. 2, no. 1, pp. 34–42, 2013.

[15] A. Guechaichia and I. Trendafilova, “A simple frequency-based delamination detection and localization method without baseline model,” *Journal of physics:Conference Series*, vol. 382, 2012, doi: 10.1088/1742-6596/382/1/012033.

[16] R. Sultan, S. Guirguis, M. Younes, and E. El-Soaly, “Effect of the thickness-wise location delamination on natural frequency for laminate composite,” *International Journal of Applied Engineering Research*, vol. 8, no. 2, pp. 157–170, 2013.

[17] J. J. Tracy and G. C. Pardoen, “Effect of delamination on the natural frequencies of composite laminates,” *J Compos Mater*, vol. 23, no. 12, pp. 1200–1215, 1989, doi: 10.1177/002199838902301201.

[18] F. Ju, H. P. Lee, and K. H. Lee, “Finite element analysis of free vibration of delaminated composite plates,” *Composites Engineering*, vol. 5, no. 2, pp. 195–209, 1995, doi: 10.1016/0961-9526(95)90713-L.

[19] D. A. Saravanos and D. A. Hopkins, “Effects of delaminations on the damped dynamic characteristics of composite laminates: Analysis and experiments,” *J Sound Vib*, vol. 192, no. 5, pp. 977–993, 1996, doi: 10.1006/jsvi.1996.0229.

[20] K. Kaware, M. Kotambkar, A. Sontakkey, and N. Talekar, “Hybridization effect of Kevlar and glass fibers on CFRP composite under low velocity impact: Numerical simulations,” *International Journal of Crashworthiness*, vol. 27, no. 4, pp. 1232–1256, 2022, doi: 10.1080/13588265.2021.1914985.

[21] K. Kaware and M. Kotambkar, “Experimental investigation of hybridization effect of Kevlar and Glass fibers on CFRP composite under low velocity impact,” *International Journal of Crashworthiness*, vol. 0, no. 0, pp. 1–11, 2023, doi: 10.1080/13588265.2023.2230634.

[22] A. Zak, M. Krawczuk, and W. Ostachowicz, “Numerical and experimental investigation of free vibration of multilayer delaminated composite beams and plates,” *Comput Mech*, vol. 26, no. 3, pp. 309–315, 2000, doi: 10.1007/s004660000178.

[23] X. H. Jian, H. S. Tzou, C. J. Lissenden, and L. S. Penn, “Damage detection by piezoelectric patches in a free vibration method,” *Journal of Composite Material*, vol. 31, no. 4, pp. 345–359, 1997.

[24] L. H. Tenek, E. G. Henneke, and M. D. Gunzburger, “Vibration of delaminated composite plates and some applications to non-destructive testing,” *Compos Struct*, vol. 23, no. 3, pp. 253–262, 1993, doi: 10.1016/0263-8223(93)90226-G.

[25] H. S. Kim, A. Chattopadhyay, and A. Ghoshal, “Dynamic analysis of composite laminates with multiple delamination using improved layerwise theory,” *AIAA Journal*, vol. 41, no. 9, pp. 1771–1779, 2003.

[26] A. Paolozzi and I. Peroni, “Experimental assessment of debonding damage in a carbon-fibre reinforced plastic sandwich panel by frequency variations,” *Compos Struct*, vol. 35, no. 4, pp. 435–444, 1996, doi: 10.1016/S0263-8223(96)00057-8.

[27] S. H. Diaz Valdes and C. Soutis, “Delamination detection in composite laminate from variations of their modal characteristics,” *J Sound Vib*, vol. 228, no. 1, pp. 1–9, 1999.

[28] S. S. Kessler, S. M. Spearing, M. J. Atalla, C. E. S. S. Cesnik, and C. Soutis, "Damage detection in composite materials using frequency response methods," *Compos B Eng*, vol. 33, pp. 87–95, 2002, doi: 10.1016/S1359-8368(01)00050-6.

[29] L. S. Penn, J. R. Jump, M. J. Greenfield, and G. E. Blandford, "Use of the free vibration spectrum to detect delamination in thick composites," *J Compos Mater*, vol. 33, no. 1, pp. 54–72, 1999, doi: 10.1177/002199839903300104.

[30] P. M. Mujumdar and S. Suryanarayan, "Flexural vibrations of beams with delaminations," *Journal ofSound and Vibration*, vol. 125, no. 3, pp. 441–461, 1988.

[31] M. Krawczuk, W. Ostachowicz, and A. Zak, "Dynamics of cracked composite material structures," *Comput Mech*, vol. 20, pp. 79–83, 1997, doi: 10.1007/s004660050220.

[32] R. P. Thornburgh and A. Chattopadhyay, "Modeling the dynamic effects of delamination in adaptive composite laminate," *43rd AIAA/ASME/ASCE/AHS/ASC Structures, Structural Dynamics and Materials Conference*, pp. 1944–1954, 2002, doi: 10.2514/6.2002-1443.

[33] H. Luo and S. Hanagud, "Delamination detection using dynamic characteristics of composite plates," *AIAA-95-1172-CP*, vol. 1, pp. 129–139, 1995, doi: 10.2514/6.1995-1172.

[34] H. Luo and S. Hanagud, "Delamination modes in composite plates," *J Aerosp Eng*, vol. 9, no. 4, pp. 106–113, 1996, doi: 10.1061/(ASCE)0893-1321(1996)9:4(106).

[35] M. H. H. Shen and J. E. Grady, "Free vibrations of delaminated beams," *AIAA Journal*, vol. 30, no. 5, pp. 1361–1370, 1992, doi: 10.2514/3.11072.

[36] W. Lestari and S. Hanagud, "Health monitoring of structures: multiple delamination dynamics in composite beams," *The American Institute of Aeronautics and Astronautics Inc.*, vol. 4, pp. 2453–2462, 1999, doi: 10.2514/6.1999-1509.

[37] H. Luo and S. Hanagud, "Delaminated beam nonlinear dynamic response calculation and visualization," *American Institute of Aeronautics and Astronautics, Inc.*, pp. 490–499, 1997, doi: 10.2514/6.1997-1159.

[38] H. Luo and S. Hanagud, "PVDF sensor and its applications in delamination response detection," *American Institute of Aeronautics and Astronautics, Inc.*, pp. 720–728, 1997, doi: 10.2514/6.1997-1218.

[39] S. Lee, T. Park, and G. Z. Voyiadjis, "Vibration analysis of multi-delaminated beams," *Compos B Eng*, vol. 34, no. 7, pp. 647–659, 2003, doi: 10.1016/S1359-8368(03)00053-2.

[40] J. F. Zhu, Y. Gu, and L. Tong, "Formulation of reference surface element and its applications in dynamic analysis of delaminated composite beams," *Compos Struct*, vol. 68, no. 4, pp. 481–490, 2005, doi: 10.1016/j.compstruct.2004.04.014.

[41] J. Lee, "Free vibration analysis of delaminated composite beams," *Comput Struct*, vol. 74, pp. 121–129, 2000, doi: 10.1145/3025171.3025210.

[42] D. Shu and C. N. Della, "Vibrations of multiple delaminated beams," *Compos Struct*, vol. 64, pp. 467–477, 2004, doi: 10.1016/j.compstruct.2003.09.047.

[43] D. Shu and C. N. Della, “Free vibration analysis of composite beams with two non-overlapping delaminations,” *Int J Mech Sci*, vol. 46, no. 4, pp. 509–526, 2004, doi: 10.1016/j.ijmecsci.2004.05.008.
[44] C. N. Della and D. Shu, “Vibration of beams with double delaminations,” *J Sound Vib*, vol. 282, pp. 919–935, 2005, doi: 10.1016/j.jsv.2004.03.052.
[45] C. N. Della and D. Shu, “Free vibration analysis of composite beams with overlapping delaminations,” *European Journal of Mechanics, A/Solids*, vol. 24, no. 3, pp. 491–503, 2005, doi: 10.1016/j.euromechsol.2005.01.007.
[46] L. H. Yam, Z. Wei, L. Cheng, and W. O. Wong, “Numerical analysis of multi-layer composite plates with internal delamination,” *Comput Struct*, vol. 82, pp. 627–637, 2004, doi: 10.1016/j.compstruc.2003.12.003.
[47] D. X. Lin, R. G. Ni, and R. D. Adams, “Prediction and measurement of the vibrational damping parameters of carbon and glass fibre-reinforced plastics plates,” *J Compos Mater*, vol. 18, no. 2, pp. 132–152, 1984, doi: 10.1177/002199838401800204.
[48] Z. Wei, L. H. Yam, and L. Cheng, “Detection of internal delamination in multi-layer composites using wavelet packets combined with modal parameter analysis,” *Compos Struct*, vol. 64, pp. 377–387, 2004, doi: 10.1016/j.compstruct.2003.09.038.